Published in final edited form as:
Biomacromolecules. 2012 May 14; 13(5): 1598–1605. doi:10.1021/bm300321n.

Unexpected multivalent display of proteins by temperature triggered self-assembly of elastin-like polypeptide block copolymers

Wafa Hassouneh[*], **Karl Fischer**[†], **Sarah R. MacEwan**[*], **Robert Branscheid**[†], **Chuan Lawrence Fu**[‡], **Rihe Liu**[‡], **Manfred Schmidt**[†], and **Ashutosh Chilkoti**[*]

[*]Department of Biomedical Engineering, Duke University, Durham, NC 27708

[†]Institute of Physical Chemistry, Johannes Gutenberg University, Mainz, Germany 55099

[‡]Eshelman School of Pharmacy and Carolina Center for Genome Sciences, University of North Carolina, Chapel Hill, NC, 27599

Abstract

We report herein the unexpected temperature triggered self-assembly of proteins fused to thermally responsive elastin-like polypeptides (ELPs) into spherical micelles. Six ELP block copolymers (ELP_{BC}) with different hydrophilic and hydrophobic block lengths were genetically fused to two single domain proteins, thioredoxin (Trx) and a fibronectin type III domain (Fn3) that binds the $\alpha_v\beta_3$ integrin. The self-assembly of these protein-ELP_{BC} fusions as a function of temperature was investigated by UV spectroscopy, light scattering, and cryo-TEM. Self-assembly of the ELP_{BC} was –unexpectedly- retained upon fusion to the two proteins, resulting in the formation of spherical micelles with a hydrodynamic radius that ranged from 24–37 nm, depending on the protein and ELP_{BC}. Cryo-TEM images confirmed the formation of spherical particles with a size that was consistent with that measured by light scattering. The bioactivity of Fn3 was retained when presented by the ELP_{BC} micelles as indicated by the enhanced uptake of the Fn3-decorated ELP_{BC} micelles in comparison to the unimer by cells that overexpress the $\alpha_v\beta_3$ integrin. The fusion of single domain proteins to ELP_{BC}s may provide a ubiquitous platform for the multivalent presentation of proteins.

Keywords

Micelle; Multivalent display; Block copolymer; Fusion protein; Elastin-like polypeptide; Targeted delivery

Introduction

Nanoparticles are currently of immense interest in medicine because of their ability to function as carriers of drugs and imaging agents.[1] They are of particular interest for imaging and therapy of solid tumors because nanoparticles ranging between 10–100 nm in size exceed the renal clearance threshold while maintaining the ability to diffuse across the leaky vasculature of tumors into the extravascular region where tumor cells reside, thereby leading to enhanced permeability and retention compared to small molecule drugs and imaging

Address correspondence to chilkoti@duke.edu.

Supporting Information Available. Additional data on temperature-programmed turbidimetry and light scattering data and analysis is available. This information is available free of charge via the Internet at http://pubs.acs.org.

agents.[1] Nanoparticles have also been decorated on their exterior with a range of targeting moieties such as proteins (e.g., antibodies or their fragments), nucleic acids (e.g., aptamers) and small molecule ligands (e.g., vitamins) to achieve enhanced cellular uptake through receptor-mediated endocytosis.[1–11] The multivalent display of these targeting moieties through presentation on the exterior of nanoparticles can result in increased avidity for their corresponding receptors, which are overexpressed on tumor cells.[12–14] Despite the great interest in using intact proteins or protein domains to target receptors *in vivo*, available platforms that can self-assemble a protein into multivalent nanoparticles require post-synthesis conjugation.

This study builds upon our previous study [15], that of Conticello and coworkers,[16,17] and Chaikof and coworkers[18] which showed that diblock polypeptides composed of two different segments of an elastin-like polypeptide (ELP) can self-assemble into micelles.[19] ELPs are repetitive biopolymers composed of the pentapeptide repeat [Val-Pro-Gly-Xaa-Gly] found in tropoelastin [20], where Xaa is a guest residue that can be any amino acid except proline.[21,22] ELPs exhibit lower critical solution temperature (LCST) transition behavior, where above a critical temperature – herein termed the inverse transition temperature (T_t)– a single segment ELP transitions from a soluble disordered chain to a collapsed insoluble aggregate. We have previously shown that ELP block copolymers (ELP_{BC}) in some cases assemble into micelles over a specific temperature range when composed of two blocks with different T_ts as controlled by their guest residue composition and block length.[15] This is because the ELP block with the lower T_t –the hydrophobic block– desolvates independently of the hydrophilic block as the temperature of the solution is increased, thereby imparting sufficient amphiphilicity to the polymer chain, which subsequently drives its self-assembly into a spherical micelle with a core composed of the hydrophobic block and a corona composed of the hydrophilic ELP block.

In a conservative extension of this study, we next showed that short peptides (≤10 amino acids) could be tolerated at the hydrophilic end of ELP_{BC}s without disrupting their self-assembly,[12] which was not entirely surprising given the relatively small size of the terminal peptide ligand appended in comparison to the ELP_{BC}s employed in these studies that are typically 600–1000 amino acids in length. These previous studies led us to speculate about the maximum size of a polypeptide moiety that could be tolerated at the terminus of the hydrophilic segment without disrupting self-assembly, and whether this system could potentially enable multivalent display of proteins on the corona of ELP_{BC} micelles (Figure 1) motivated by the recognition that this would provide a completely genetically encoded system for the multivalent display of protein targeting ligands.

Herein, we present the unexpected finding that intact proteins – comprising 95–110 residues and that are significantly larger than the short peptides previously used– can be tolerated in the corona of ELP_{BC} micelles, suggesting a large degree of structural flexibility in their self-assembly. Notably, one of the proteins that displayed self-assembly is an engineered fibronectin type III domain (Fn3) that provides a small (compared to intact antibodies), easy to express in *Escherichia coli* (*E. coli*), and structurally stable alternative to antibodies for targeting. Fn3 can be engineered by directed evolution to bind to diverse receptors, thereby potentially providing a genetically encoded nanoparticle system that could be engineered to target a variety of cell surface receptors of interest in medicine.[23,24]

Methods

ELP cloning and expression

A set of six ELP_{BC} genes previously constructed in our group provided the starting point for the synthesis of the protein-ELP_{BC} fusions.[15] These ELP_{BC}s have a guest residue

composition of valine, glycine and alanine at a ratio of 1:7:8 for the hydrophilic block and valine for the hydrophobic block. Here we indicate the block length in pentapeptide repeats. The ELP_{BC}s are identified by the length of each of the two blocks using the following nomenclature: "ELP *m*–*n*" where *m* and *n* are the hydrophilic and hydrophobic block lengths, respectively, as number of VPGXG repeats. For example ELP 96-90 has a hydrophilic block of 96 pentapeptides and a hydrophobic block of 90 pentapeptides. The block lengths (i.e. number of pentapeptide repeats) for the hydrophilic and hydrophobic blocks respectively were: 64-60; 64-90; 64-120; 96-60; 128-60; 96-90. The gene encoding *E. coli* Trx was obtained from the vector pET-32a (Novagen) while the Fn3 gene against $\alpha_v\beta_3$ was available from a previous study.[24] The two genes were amplified using PCR with primers encoding for the NdeI site at each end. The amplified genes were digested using the NdeI restriction enzyme (NEB) and ligated to each of the ELP_{BC} vectors that had also been digested with the same restriction enzyme and subsequently dephosphorylated using calf intestine phosphatase (CIP) (NEB). The resulting colonies were screened using colony PCR. The successfully sequenced clones were transformed into BL21(DE3) *E. coli* cells. The BL21(DE3) cells with the constructed plasmids were grown in 1 liter of terrific broth for 24 hours. The proteins were extracted and purified as described in Meyer et al. [25,2625,26] The ELP_{BC} was used as a purification tag for the proteins and inverse transition cycling (ITC) was used to separate the protein-ELP_{BC} fusion from contaminants. The purity of the samples was verified by visualization using sodium dodecyl sulfate polyacrylamide gel electrophoresis (SDS-PAGE).

Thermal characterization

The thermal characteristics of the protein-ELP_{BC} fusions were investigated using a UV-Vis spectrophotometer (Cary 300 Bio; Varian Inc., Cary, NC). The samples were heated at a rate of 1 °C/min as absorbance measurements were recorded at 0.3 °C intervals. The samples were prepared in PBS at a concentration of 25μM.

Dynamic and static light scattering (DLS/SLS)

Hydrodynamic radii were measured at different temperatures using a temperature controlled DLS instrument (DynaPro, Wyatt technologies, Santa Barbra, CA). A single detector at 90° measured intensity fluctuations as the temperature was increased in 1 °C increments. Three readings per minute were recorded at each temperature.

DLS/SLS measurements were performed using the ALV/CGS-3 goniometer system or the ALV/CGS-8F platform based goniometer system. Measurements on the ALV/CGS-8F system were performed at Johannes Gutenberg University in Mainz, Germany. Samples for the ALV/CGS-8F goniometer system were prepared by filtering solutions of the protein-ELP_{BC} fusions through an Anatop 10 Whatman 20nm filter using a Luer lock syringe (10mL, Hamilton, Reno, NV) into a quartz glass 20mm-diameter cylindrical cuvette (custom designed SUPRASIL quartz, Hellma, Müllheim, Germany). Filtration was carried out in a laminar flow cabinet. The cuvettes were precleaned using a refluxing acetone fountain to remove dust. ALV/CGS-8F is a multi-detector system with 8 detectors set 17° apart. The SLS measurements were set up so that the first detector moved from 25° to 39.875° in 2.125° steps. The DLS measurements were set up so that the first detector moved from 30° to 39° in one step. DLS measurements were done in 5 runs, 60 seconds each at each angle. SLS measurements were done in 10 runs, 10 seconds each at each angle. The refractive index increment was estimated to be 0.186 cm^3/g.[27,28] Correlation function analysis was performed by a Simplex routine utilizing a biexponential fit, from which the initial slope, i.e. the first cumulant, was calculated. A very small (less than 5%) but significant negative slope of the apparent diffusion coefficient versus q^2 was observed for some of the micelle solutions. A closer inspection revealed that this effect most likely originates from the onset

of multiple scattering which is known to add a fast mode to the correlation function at small q.[29] Upon modification of the data analysis by fitting the correlation function from a point where the fast mode has already decayed, i.e. from 90–80% down to 10–15% (but avoiding unphysical systematic negative residues), the negative slope disappeared and an almost q-independent apparent diffusion coefficient was observed (see Supp Figure 6–15 for details). It should be noted that intermolecular electrostatic interaction as an alternative source of the negative slope of D_{app} versus q^2 can be safely excluded since control experiments at 0.14 M NaCl, where electrostatic interactions are screened, did also show a negative slope.

Samples for the ALV/CGS-3 goniometer system were prepared by filtering solutions of the protein-ELP_{BC} fusions through an Anatop 10 Whatman 20 nm filter into a 10 mm disposable borosilicate glass tube (Fischer). The tube was pre-cleaned by washing three times with filtered ethanol (0.2 μm cellulose acetate filter). Simultaneous SLS/DLS measurement were obtained for angles between 30°–150° at 5° increments done in 3 runs each 30 seconds at each angle.

Cryo-transmission electron microscopy (Cryo-TEM)

A 25 μM sample of Trx-ELP 96,90 was vitrified in liquid propane using the climate chamber of a Vitrobot® (FEI, Eindhoven, Netherlands) at 55 °C and 80% humidity. The cryo-TEM measurements were performed with Philips CM12 at 120 kV (FEI, Eindhoven, Netherlands). The images were obtained at Johannes Gutenberg University in Mainz, Germany

Fluorophore conjugation—To detect cellular uptake of Fn3 micelles by tumor cells, Alexa Fluor® 488 sulfodichlorophenol ester dye (Invitrogen) was conjugated to Fn3-ELP 96-90 or the control of ligand-negative ELP 96,90 by reacting the dye to the lysine residues present in either construct. A 25μM solution of each sample was prepared. Within one ITC round, the samples were resuspended in 0.1 M sodium bicarbonate buffer, pH 8.3. The reaction was carried out according to the instructions of the supplier. After the reaction was completed, a round of ITC was used to separate the ELP constructs from unreacted dye. The samples were further purified using PD-10 Sephadex™ G-25 M columns (GE healthcare). Once the degree of labeling was calculated, the two samples (Fn3-ELP 96-90 and ELP 96-90) were mixed with the corresponding unlabeled constructs to obtain the same degree of labeling for both samples. The labeled constructs were characterized through temperature controlled absorbance measurements as well as DLS measurements to ensure that they retained self-assembly behavior.

Cell culture—Two tumor cell lines, wild type K562 (K562/WT) and K562 that overexpress the $\alpha_v\beta_3$ integrin (K562/$\alpha_v\beta_3$), were available from previous studies.[24] The cell lines were cultured in RPMI 1640 media (Invitrogen) supplemented with 10% FBS and 1% penicillin/streptomycin. The K562/$\alpha_v\beta_3$ media also contained 500 μg/mL G418 (Invitrogen). The cell cultures were maintained at 37°C and 5% CO_2. Cell cultures were started from frozen stocks and were split every 48 hrs.

Cell uptake—A total of 500,000 K562/WT or K562/$\alpha_v\beta_3$ cells were plated in 6-well plates and allowed to incubate overnight. The cells were rinsed twice and resuspended in 500 μL of 10μM Fn3-ELP 96-90-Alexa488 or ELP 96-90-Alexa488 in Hank's balanced salt solution (HBSS). The cells were incubated at either room temperature (below critical micelle temperature (CMT)) or 38 °C (above CMT) in normal atmosphere for 1 hour. The cells were then rinsed twice in binding buffer. Cells for flow cytometry were fixed in 4% PFA for 20 min and stored at 4 °C.

Flow cytometry—Cell samples were analyzed using a LSRII Flow cytometer (BD Biosciences, San Jose, CA). Viable cells were gated using the forward and side scatter plots of unstained control cells. 10,000 cells were analyzed for each sample. Fold increase in median fluorescence was calculated by dividing the median of the cell fluorescence intensity histogram above the CMT by that below the CMT for a given sample (Fn3-ELP 96-90 or ELP 96-90) and cell line (K562/WT or K562/$\alpha_v\beta_3$).

Results and Discussion

A set of ELP_{BC}s that were previously shown to self-assemble into spherical micelles was chosen for fusion to two proteins.[15] The set includes six block copolymers that differ from each other in the length of each block and the ratio of the lengths of the two blocks. The hydrophilic block contained the guest residues valine, glycine and alanine in a ratio of 1:7:8, while the hydrophobic block solely contained valine as the guest residue. The ELP_{BC}s are identified by the length of each of the two blocks using the following nomenclature: "ELP *m*–*n*" where *m* and *n* are the hydrophilic and hydrophobic block lengths, respectively, as number of VPGXG repeats.

We selected two proteins for this initial study of the effect of proteins on ELP_{BC} self-assembly: thioredoxin (Trx) and a fibronectin type III domain (Fn3). While both proteins are relatively small single domain proteins with a molecular weight (MW) of ~10 kDa, we chose them as they have significantly different surface properties, as determined by the computational method described in Trabbic-Carlson et al.[30] Trx was chosen because it is a small, stable, and soluble model protein that expresses well as a fusion with ELP.[25]

We were specifically intrigued by the prospect of Fn3 as the second protein for a number of reasons: First, Fn3 has a similar size as Trx but is more hydrophobic. Second, the specific Fn3 domain that we chose for this study targets the $\alpha_v\beta_3$ integrin, which is over-expressed by tumor endothelial cells and is hence of interest to target the tumor vasculature.[12, 13] Third, the Fn3 domain can be engineered at its binding loops to impart affinity to a variety of targets rendering it a versatile protein scaffold that provides an alternative to antibodies and their fragments. [31, 32] Despite the great interest in using Fn3 domains as antibody mimics, their low molecular weight dictates that these fragments have a short half-life in circulation, so that the major advantage of smaller size –better tissue penetration[33]– is abrogated by their poor residence time *in vivo*. Methods to increase their half-life, such as their presentation by polymer micelles are hence of interest, and provided additional motivation to select this protein beyond the prospect of increasing their "avidity" for their receptor of interest via multivalency. [31,34] Fourth, this protein has exceptionally high thermal stability, with a melting temperature of ~ 90 °C, so that varying the solution temperature to drive self-assembly would be unlikely to thermally denature the protein.[24]

The two proteins, Trx and Fn3, were fused to the six ELP_{BC}s at the gene level, and plasmid-borne copies of the genes of each of these fusions were expressed in *E. coli* to synthesize the protein-ELP_{BC} fusions for the studies described herein. After purification of each construct to homogeneity, their temperature-triggered self-assembly was characterized by temperature-programmed UV-Vis spectroscopy, light scattering, and cryo-TEM.

Thermal properties of protein-ELP_{BC} fusions

The thermal properties of the protein-ELP_{BC} fusions were determined by monitoring their absorbance at 350 nm while heating the sample at a rate of 1°C/min. Single segment ELPs show a single sharp step increase in absorbance indicative of a unimer-to-aggregate transition.[35] ELP_{BC}s that undergo self-assembly exhibit a three state behavior: unimer, nanoparticle and aggregate, which is reflected by differences in their absorbance with

increasing temperature as compared to single segment ELPs. A slight increase in absorbance (~0.1–0.5 OD_{350}) is observed indicating nanoparticle formation as the ELP_{BC} transitions from unimer to micelle upon the collapse of the hydrophobic block with an increase in solution temperature.[15] The temperature at which the unimer-to-micelle transition occurs is termed the critical micelle temperature (CMT). As the solution is heated further above the CMT, the ELP_{BC} eventually transitions from a micellar phase to micron-sized aggregates upon the collapse of the hydrophilic block, which is indicated by a much larger increase in absorbance (OD_{350} ~2 for a 25 μM solution of a typical ELP_{BC}). Surprisingly, similar to the ELP_{BC} control, both the Trx- and Fn3-ELP_{BC} fusions retained the three-state behavior of the ELP_{BC} (Figures 2 and 3) as indicated by the similar pattern of changes in absorbance with increasing temperature. Both transitions were reversible for temperature ranges below the respective protein's denaturation temperature.

The protein-ELP_{BC} fusions showed consistent trends in their unimer-to-micelle and micelle-toaggregate transition temperatures based on block lengths (Figure 2A and Figure 3A). Figure 2A shows the thermal profiles of three Trx-ELP_{BC} fusions with increasing hydrophobic block lengths (60, 90 and 120 pentapeptide repeats). Increasing the hydrophobic block length decreased the unimer-to-micelle transition temperature as consistent with the effect of increased length in decreasing ELP T_t.[35] Similarly, Figure 3A shows the thermal profiles of Fn3 fused to the same three ELP_{BC}s. The same effect on the unimer-to-micelle transition temperature with increasing hydrophobic block lengths was observed. However, increasing the hydrophilic block length showed opposite trends for the hydrophobic (Fn3) vs. the hydrophilic (Trx) protein (Supp Figure 1 and 2). For Trx, increasing the hydrophilic block lengths (64, 96, and 128 pentapeptides) resulted in lower micelle-to-aggregate transition temperatures, which is also consistent with the effect of increased length on ELP T_t. For Fn3, increasing the hydrophilic block lengths resulted in higher micelle-to-aggregate transition temperatures. We hypothesize that this unexpected effect may be related to the hydrophobicity of the protein, such that each protein has different interaction strengths with the two ELP blocks. This hypothesis will be tested in future work.

For both proteins, the unimer-to-micelle transition temperature –the CMT– did not change compared to that of the corresponding free ELP_{BC}, suggesting that the fused proteins did not have an effect on the hydrophobic block transition temperature. However, fusion of these proteins to the ELP_{BC}s had a significant effect on the adjacent hydrophilic block transition temperature. The more hydrophobic protein, Fn3, depressed the hydrophilic block transition temperature while the more hydrophilic protein, Trx, elevated the transition temperature (Supp Figure 3). These results agree with the previously observed "ΔT_t effect" of proteins fused to a single ELP segment wherein the fused protein increases or decreases the T_t of an ELP depending on whether its surface area is hydrophilic or hydrophobic relative to that of the ELP.[30] These results are hence consistent with the notion that the surface properties of the fused protein affect the phase behavior of the adjacent ELP to which the protein is fused.

Dynamic and static light scattering

The two sets of protein-ELP_{BC} fusions were further characterized by light scattering. The apparent diffusion coefficient of particles was determined by dynamic light scattering (DLS), and the hydrodynamic radius (R_h) was calculated from the diffusion coefficient using the Stokes-Einstein equation.[36] R_h was determined as the temperature was increased in 1 °C increments. The measured R_h and the change in absorbance for Trx-ELP 96-90 and Fn3-ELP 96-90 are shown in Figure 2b and Figure 3b, respectively. The change in R_h with solution temperature confirms three-state behavior. Below the CMT, the protein-ELP_{BC} fusions are unimers with R_h in the range of 6–7.5 nm. Above their CMT, the protein-ELP_{BC}

fusions formed monodisperse nanoparticles with R_h in the range of 24–36.6 nm depending on the protein and ELP_{BC}. Similarly, upon further increase in temperature past the CMT, the collapse of the hydrophilic block resulted in the formation of micron-sized aggregates. These aggregates were first detected by DLS at the same temperature at which the large step increase in absorbance occurred (DLS data for the aggregates is not shown, as they are highly polydisperse micron-sized particles). The DLS measurements also showed no significant changes in R_h with increasing temperature over the temperature range in which nanoparticles were detected. The effect of concentration on the R_h of protein-ELP_{BC} micelles was also investigated for Trx-ELP 96-90. No significant change in the R_h was observed over a range of concentrations above the critical micelle concentration (CMC) (Supp Figure 4). When R_h was measured at a range of scattering angles, the apparent diffusion coefficient showed no dependence on angle, which indicated that the particles were monodisperse and spherical (Supp Figure 5A).[36]

To further characterize the structure of the self-assembled nanoparticles, static light scattering (SLS) was carried out. By measuring the intensity of scattered light as a function of scattering angle, a Zimm plot was constructed (Supp figure 5B). Using the equation below, the radius of gyration (R_g) and the molecular weight of the particle (M_W) was calculated from the slope and intercept of a linear fit respectively.[36]

$$\frac{Kc}{R} = \frac{1}{M_w} + \frac{1}{3}\frac{1}{M_w} q^2 R_g^2$$

where R is the Raleigh ratio, q is the scattering wave vector (related to angle), c is the concentration of the sample, and K is the optical constant. The properties of the nanoparticles formed by the two sets of protein-ELP_{BC} fusions are summarized in Table 1. The molecular weight of the particle allows calculation of the aggregation number (i.e., number of unimers per micelle). The aggregation numbers in Table 1 are not corrected for the CMC, which indicates that the calculated numbers are minimum aggregation numbers and, in reality, could be larger. The apparent aggregation numbers of both sets range from 25 to 150 unimers/micelle, which is typical for micelles. The R_g was used to determine the ratio of R_h to R_g, known as ρ, which is indicative of the topology of the particle. Theoretically, a hard uniform sphere has a ρ value of 0.775; a hollow sphere has a ρ value of 1; and a random coil has a ρ value of 1.5.[36] Lower ρ values than the theoretical hard sphere ρ value are often observed for soft spherical particles such as micelles[37,38] and collapsed coils.[39] Trx-ELP_{BC} nanoparticles had ρ values of 0.6–0.82 and Fn3 ELP_{BC} nanoparticles had ρ values of 0.6–0.74. These values indicate the formation of soft spherical micelles by both protein-ELP_{BC} fusions.

To directly visualize the self-assembled structures, cryo-TEM images of Trx-ELP 96-90 micelles were obtained for samples prepared at 55 °C, which for this construct is above its CMT (Figure 4). The images show spherical particles of ~50 nm in diameter, which corresponds to the measured hydrodynamic diameter of 61.2 nm for this construct.

Cellular uptake

To assess the bioactivity of the proteins when presented in the form of protein-ELP_{BC} micelles, flow cytometry was used to evaluate the binding of fluorescently labeled Fn3-ELP 96-90 to the $\alpha_v\beta_3$ integrin. A transfected human leukemia cell line, K562, that overexpresses the $\alpha_v\beta_3$ integrin (K562/$\alpha_v\beta_3$) was available from previous studies,[24] as was the wild-type (WT) cell line that exhibits low baseline expression of this integrin (K562/WT). The binding of Fn3-ELP 96-90 was measured below and above the CMT (room

temperature and 38 °C respectively) to determine the effect of micellar presentation of the Fn3 domain on cell uptake in comparison to the unimeric form. ELP 96-90 was also used as a ligand-negative ELP control to measure the nonspecific cell uptake of ELP micelles.

The fluorescence intensity histogram of K562/$\alpha_v\beta_3$ cells showed a shift towards more fluorescent cells when they were incubated with Fn3-ELP_{BC} micelles as compared to unimers (Figure 5A-1) indicating that multivalent display of the Fn3 domain by micelles is more effective at promoting cell uptake than the unimers. Interpretation of this result is however convoluted by two effects: the effect of self-assembly of the ELP_{BC} into a micelle and that of multivalent presentation of the protein ligand. To deconvolute these effects, cell uptake by K562/$\alpha_v\beta_3$ cells was compared for Fn3-ELP 96-90 micelles with the ligand-negative ELP 96-90 micelles (Figure 5A-2). Fn3-ELP_{BC} micelles showed significantly greater uptake as compared to the ligandnegative ELP_{BC} micelles, indicating that the effect observed in Figure 5A-1 is largely due to the multivalent presentation of the Fn3 domain, rather than the self-assembly of the ELP_{BC} into micelles. Integrin-mediated uptake was also confirmed by using the receptor-negative WT K562 cell line that does not overexpress the $\alpha_v\beta_3$ integrin. A significant increase in fluorescence intensity was observed when Fn3-ELP 96-90 micelles were incubated with K562/$\alpha_v\beta_3$ cells in comparison to unmodified K562/WT cells (Figure 5A-3). These findings confirm that highest uptake occurs when cells overexpressing the $\alpha_v\beta_3$ integrin are incubated with ELP_{BC} micelles that present multiple copies of the Fn3 domain.

The fold increase of the median fluorescent intensities of K562/$\alpha_v\beta_3$ and K562/WT cells incubated with Fn3-ELP 96-90 and ELP 96-90 above the CMT, compared to that below the CMT, is plotted in Figure 5B. No significant difference was observed between the two cell lines (K562/WT and K562/$\alpha_v\beta_3$) incubated with ELP 96-90. However, a significant difference in the fold-increase was observed for the cell lines incubated with Fn3-ELP 96-90; twice the fold increase is observed for K562/$\alpha_v\beta_3$ cells compared to K562/WT indicating enhanced uptake in the presence of the Fn3 domain. These results clearly show that the Fn3 domain presented on the micelle is bioactive and exhibits enhanced targeting and uptake as compared to its unimer form and the ligand-negative ELP_{BC} control micelle.

Conclusions

Herein, we have demonstrated the potential of a genetically encoded polypeptide platform in which proteins can be uniformly displayed on the exterior of a self-assembled nanoparticle without the need for covalent attachment chemistry. The genes of two proteins were seamlessly fused to that of an ELP_{BC} creating one genetically encoded construct that was recombinantly expressed as one unit thereby linking the protein covalently to the end of an ELP. Self-assembly of the fusion in response to an increase in solution temperature creates a nanoparticle – specifically a spherical micelle– wherein the particle topology positions multiple copies of the protein at the periphery of the corona of the micelle. The protein surface properties were observed to have an effect on the temperature range in which micelles form by influencing the T_t of the hydrophilic block. These protein-ELP_{BC} micelles showed enhanced receptor-mediated cell uptake compared to that of the protein-ELP_{BC} in its unimer state and ligand-negative ELP_{BC} micelles. In contrast to previous studies that only demonstrated the presentation of short (<10 amino acid long) peptides on the corona of an ELP micelles, this study shows that the ELP_{BC} system is robust enough in its propensity for temperature-triggered self-assembly to permit the presentation of intact proteins.

These results are notable for several reasons: first, ELPs are genetically encoded, so that the fusion of the protein and ELP can be expressed from a single gene resulting in a covalently linked product with an exact molecular weight and perfect monodispersity[25] thus

eliminating the need for post-expression conjugation chemistry to append the protein targeting ligand to the surface of a nanoparticle. Second, these results suggest that a large number of small protein scaffolds of interest as targeting ligands (such as engineered minimized antibody domains [2,40] and antibody mimics [41–43]) could be multivalently presented on the exterior of these nanoparticles, whose dimensions can be tightly controlled both by the design of the ELP_{BC} and its monodispersity.

Although these studies are encouraging, several outstanding questions remain: (1) what are the physical rules governing the self-assembly of proteins fused to ELP_{BC}s?; (2) how general is this process likely to be in terms of the proteins that can be self-assembled into nanoparticles by their display on an ELP scaffold? Future studies will attempt to answer these questions.

Supplementary Material

Refer to Web version on PubMed Central for supplementary material.

Acknowledgments

This work was supported by NIH grant 2R01-GM061232-09 and 3R01-GM-061232-08S1 and by the NSF's Research Triangle MRSEC (DMR-1121107)

References

1. Davis ME, Chen ZG, Shin DM. Nat Rev Drug Discov. 2008; 7:771–782. [PubMed: 18758474]
2. Allen TM. Nat Rev Cancer. 2002; 2:750–763. [PubMed: 12360278]
3. Jule E, Nagasaki Y, Kataoka K. Bioconjug Chem. 2003; 14:177–186. [PubMed: 12526707]
4. Bae Y, Jang WD, Nishiyama N, Fukushima S, Kataoka K. Mol Biosyst. 2005; 1:242–250. [PubMed: 16880988]
5. Hong S, Leroueil PR, Majoros IJ, Orr BG, Baker JR Jr, Banaszak Holl MM. Chem Biol. 2007; 14:107–115. [PubMed: 17254956]
6. Peer D, Karp JM, Hong S, Farokhzad OC, Margalit R, Langer R. Nat Nanotechnol. 2007; 2:751–760. [PubMed: 18654426]
7. Sutton D, Nasongkla N, Blanco E, Gao J. Pharm Res. 2007; 24:1029–1046. [PubMed: 17385025]
8. Dirks AJ, Nolte RJM, Cornelissen JJLM. Advanced Materials. 2008; 20:3953–3957.
9. Reulen SW, Dankers PY, Bomans PH, Meijer EW, Merkx M. J Am Chem Soc. 2009; 131:7304–7312. [PubMed: 19469576]
10. Wang J, Tian SM, Petros RA, Napier ME, DeSimone JM. Journal of the American Chemical Society. 2010; 132:11306–11313. [PubMed: 20698697]
11. Kaufmann D, Weberskirch R. Macromol Biosci. 2006; 6:952–958. [PubMed: 17099868]
12. Simnick AJ, Valencia CA, Liu R, Chilkoti A. ACS Nano. 2010; 4:2217–2227. [PubMed: 20334355]
13. Ruoslahti E, Bhatia SN, Sailor MJ. J Cell Biol. 188:759–768. [PubMed: 20231381]
14. Mammen M, Choi SK, Whitesides GM. Angew Chem Int Edit. 1998; 37:2755–2794.
15. Dreher MR, Simnick AJ, Fischer K, Smith RJ, Patel A, Schmidt M, Chilkoti A. J Am Chem Soc. 2008; 130:687–694. [PubMed: 18085778]
16. Lee TAT, Cooper A, Apkarian RP, Conticello VP. Advanced Materials. 2000; 12:1105.
17. Sallach RE, Wei M, Biswas N, Conticello VP, Lecommandoux S, Dluhy RA, Chaikof EL. Journal of the American Chemical Society. 2006; 128:12014–12019. [PubMed: 16953644]
18. Kim W, Thevenot J, Ibarboure E, Lecommandoux S, Chaikof EL. Angew Chem Int Edit. 2010; 49:4257–4260.
19. Rabotyagova OS, Cebe P, Kaplan DL. Biomacromolecules. 2011; 12:269–289. [PubMed: 21235251]

20. Urry DW. J Protein Chem. 1984; 3:403–436.
21. McPherson DT, Xu J, Urry DW. Protein Expression and Purification. 1996; 7:51–57. [PubMed: 9172783]
22. Urry DW, Gowda DC, Parker TM, Luan CH, Reid MC, Harris CM, Pattanaik A, Harris RD. Biopolymers. 1992; 32:1243–1250. [PubMed: 1420991]
23. Koide S, Koide A, Lipovsek D. Methods Enzymol. 2012; 503:135–156. [PubMed: 22230568]
24. Duan J, Wu J, Valencia CA, Liu R. Biochemistry. 2007; 46:12656–12664. [PubMed: 17929945]
25. Meyer DE, Trabbic-Carlson K, Chilkoti A. Biotechnol Prog. 2001; 17:720–728. [PubMed: 11485434]
26. Meyer DE, Chilkoti A. Nature Biotechnology. 1999; 17:1112–1115.
27. Ball V, Ramsden JJ. Biopolymers. 1998; 46:489–492.
28. Wen J, Arakawa T, Philo JS. Analytical Biochemistry. 1996; 240:155–166. [PubMed: 8811899]
29. Segre PN, Vanmegen W, Pusey PN, Schatzel K, Peters W. J Mod Optic. 1995; 42:1929–1952.
30. Trabbic-Carlson K, Meyer DE, Liu L, Piervincenzi R, Nath N, LaBean T, Chilkoti A. Protein Eng Des Sel. 2004; 17:57–66. [PubMed: 14985538]
31. Bloom L, Calabro V. Drug Discov Today. 2009; 14:949–955. [PubMed: 19576999]
32. Richards J, Miller M, Abend J, Koide A, Koide S, Dewhurst S. J Mol Biol. 2003; 326:1475–1488. [PubMed: 12595259]
33. Dreher MR, Liu WG, Michelich CR, Dewhirst MW, Yuan F, Chilkoti A. J Natl Cancer I. 2006; 98:335–344.
34. Binz HK, Amstutz P, Pluckthun A. Nat Biotech. 2005; 23:1257–1268.
35. Meyer DE, Chilkoti A. Biomacromolecules. 2004; 5:846–851. [PubMed: 15132671]
36. Schärtl, W. Light Scattering from Polymer Solutions and Nanoparticle Dispersions. Springer; 2007.
37. Antonietti M, Bremser W, Schmidt M. Macromolecules. 1990; 23:3796–3805.
38. Antonietti M, Heinz S, Schmidt M, Rosenauer C. Macromolecules. 1994; 27:3276–3281.
39. Wu C, Wang XH. Phys Rev Lett. 1998; 80:4092–4094.
40. Carter P. Nature Reviews Cancer. 2001; 1:118–129.
41. Binz HK, Amstutz P, Pluckthun A. Nature Biotechnology. 2005; 23:1257–1268.
42. Skerra A. Curr Opin Biotech. 2007; 18:295–304. [PubMed: 17643280]
43. Holt LJ, Herring C, Jespers LS, Woolven BP, Tomlinson IM. Trends Biotechnol. 2003; 21:484–490. [PubMed: 14573361]

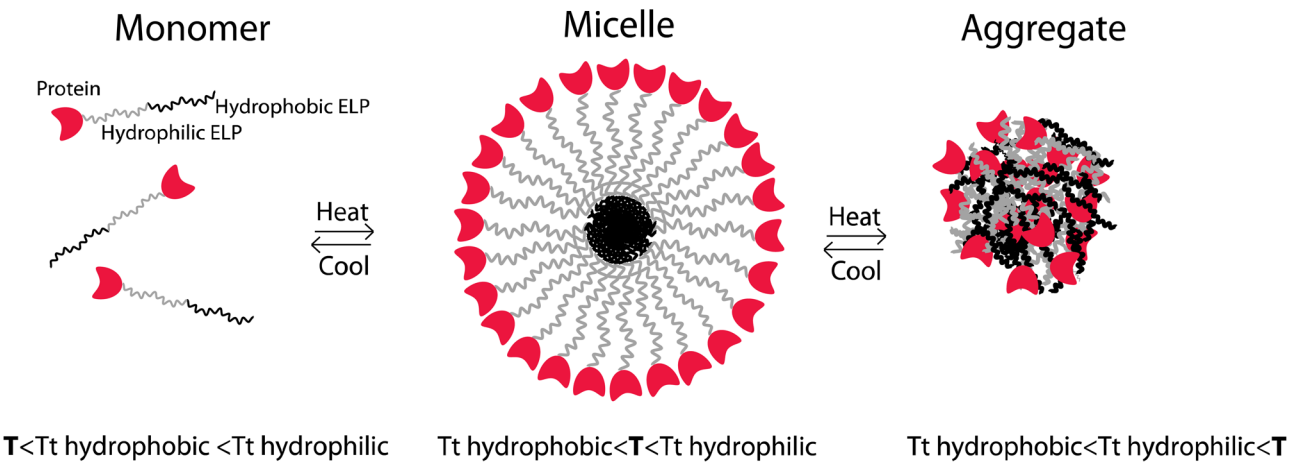

Figure 1.

Schematic of expected three state behavior of protein-ELP_{BC} fusion (the figure is not drawn to scale). Below the transition temperature of both blocks, the protein-ELP_{BC} fusion exists as a unimer. When the temperature of the solution is raised above the T_t of the hydrophobic block, it collapses and forms the core of a micelle while the hydrophilic block forms the corona. The protein, which is fused at the end of the hydrophilic block, is displayed multivalently at the exterior of the micelle. When the temperature is raised above the T_t of both blocks, a polydisperse micron-sized aggregate is formed.

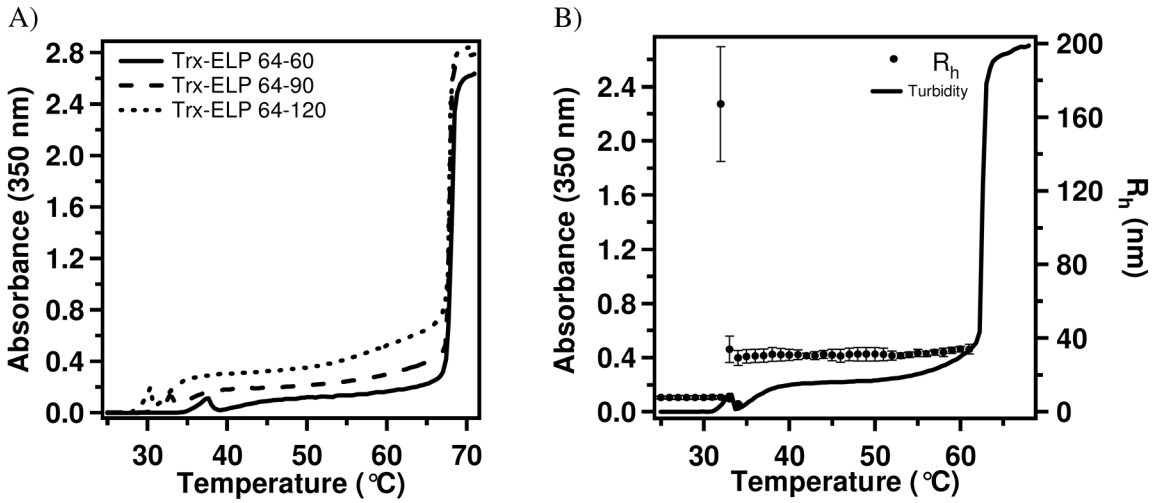

Figure 2.

A Turbidity profile of Trx-ELP_{BC} fusion with 64 pentapeptide repeats of the hydrophilic block and increasing lengths of the hydrophobic block (60, 90, and 120 pentapeptide repeats). Turbidity profiles were obtained by monitoring the absorbance of a 25 μM solution of the fusion in PBS at 350 nm while heating the samples at a rate of 1 °C/min. The unimer-to-micelle transition occurs at lower temperatures with increasing hydrophobic block lengths. The micelle-to-aggregate transition is unaffected by the length of the hydrophobic block. **B.** Turbidity profile and R_h of Trx-ELP 96-90 fusion at 25 μM in PBS. The DLS data shows the change in R_h with increasing temperature. The turbidity profile correlates with the change in R_h. The unimer, with R_h of 7 nm, transitions into a micelle, with R_h of 31 nm, at 35 °C. The R_h of the micelle is constant until the micelle-aggregate transition at ~62 °C.

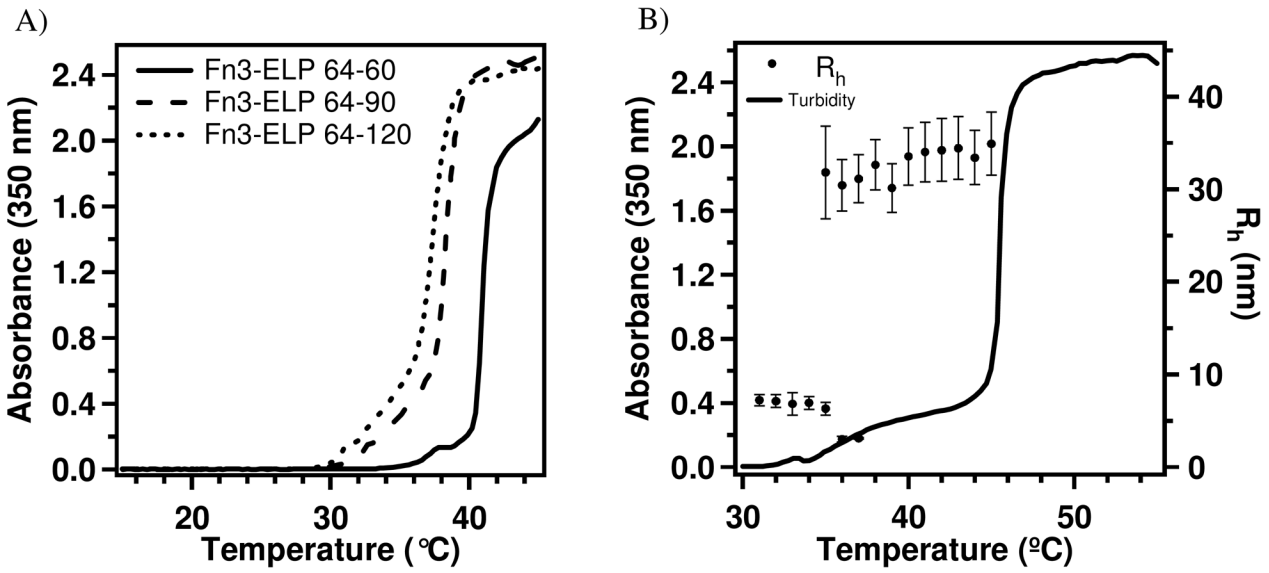

Figure 3.

A Turbidity profile of Fn3-ELP$_{\mathbf{BC}}$ fusion with 64 pentapeptide repeats of the hydrophilic block and increasing lengths of the hydrophobic block (60, 90, and 120 pentapeptide repeats). Turbidity profiles were obtained by monitoring the absorbance of a 25 μM solution of the fusion in PBS at 350 nm while heating the samples at a rate of 1 °C/min. The unimer-to-micelle transition is affected by the length of the hydrophobic block; the transitions occur at lower temperatures with increasing length of the hydrophobic block. **B.** Turbidity profile and R_h of Fn3-ELP 96-90 at 25 μM in PBS. The DLS data shows the change in R_h with increasing temperature. The turbidity profile correlates with the change in R_h. The unimer, with R_h of 7 nm, transitions into a micelle, with R_h of 35 nm, at 38 °C.

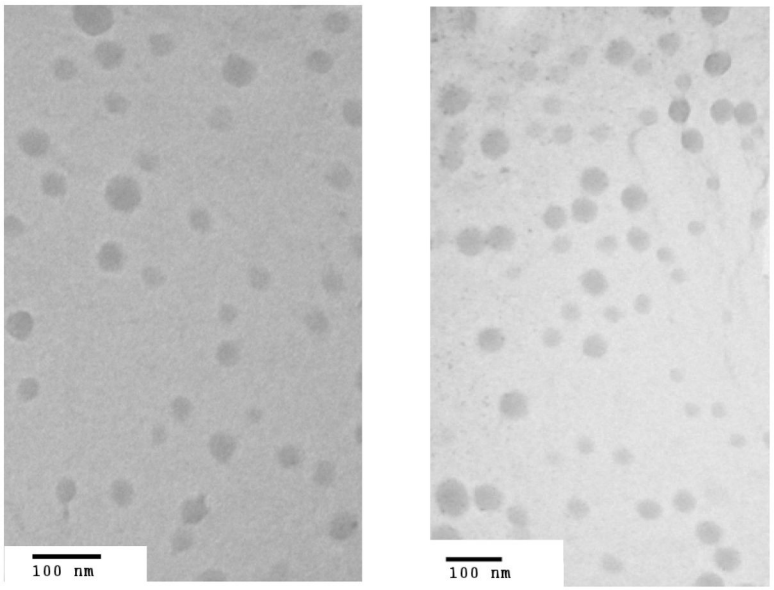

Figure 4.

Cryo-TEM images of Trx-ELP 96-90. Images were obtained for samples in PBS at 25 μM vitrified at 55 °C to induce micelle formation. These representative images show spherical particles with diameters of ~ 40–60 nm, which agree with the measured R_h of 60 nm for this sample.

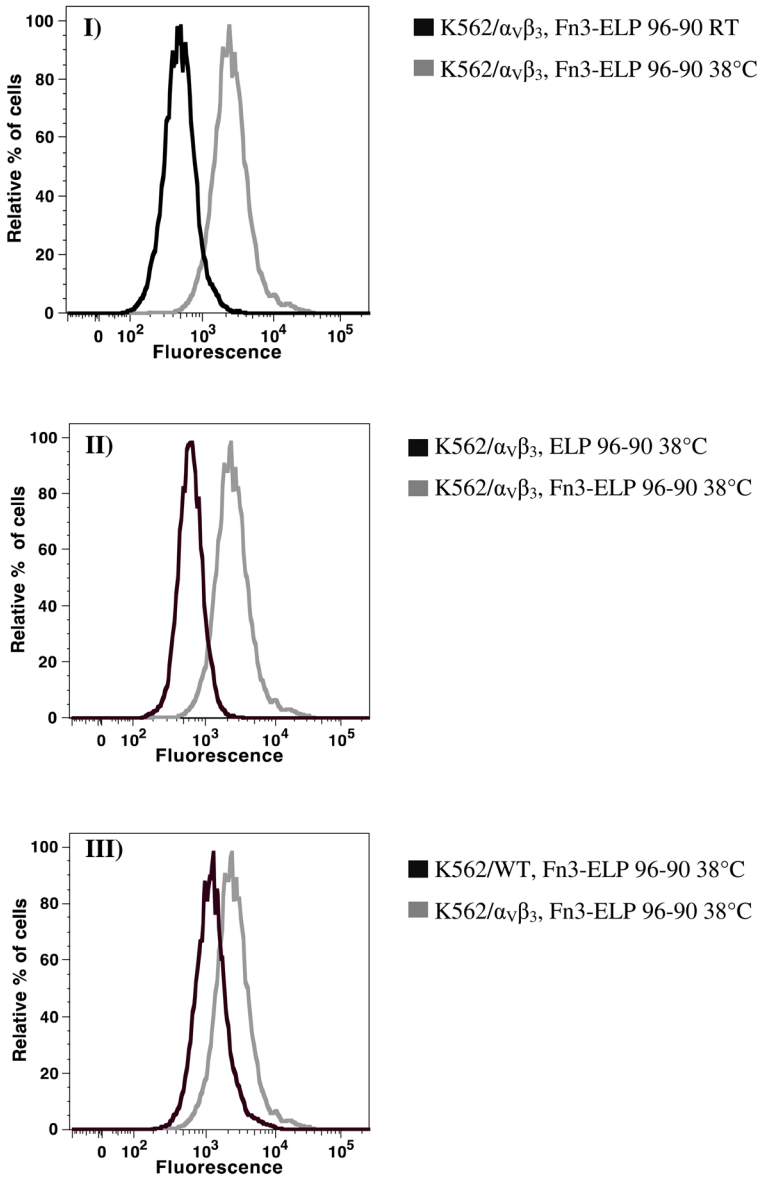

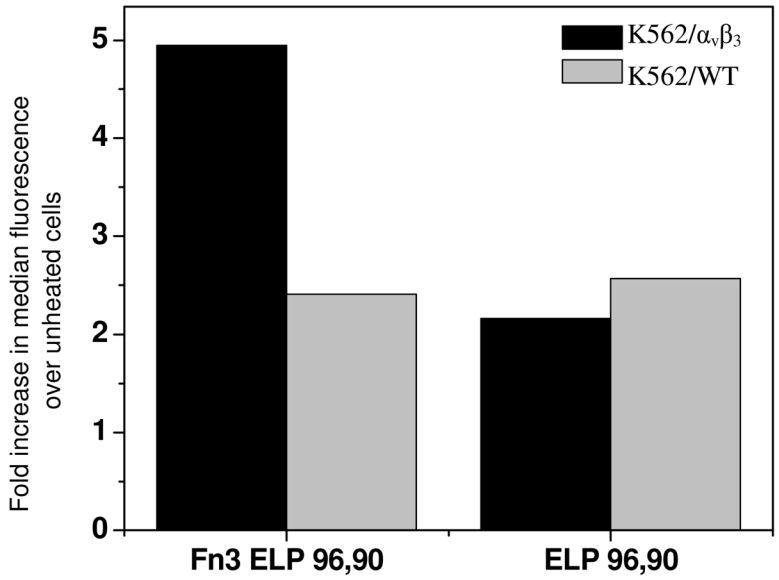

Figure 5.

Figure 5A. Flow cytometry analysis of K562/WT and K562/$\alpha_V\beta_3$ cells following incubation with 10 μM Fn3-ELP 96-90 or ELP 96-90, above and below the CMT. Panel 1 shows the histograms of K562/$\alpha_V\beta_3$ cells incubated with Fn3-ELP 96-90 above (gray) and below (black) the CMT. A shift in the median fluorescence is observed indicating enhanced uptake of Fn3-ELP 96-90 micelles compared to unimers. Panel 2 shows the histograms of K562/$\alpha_V\beta_3$ cells incubated with Fn3-ELP 96-90 micelles (gray) and ligand-negative ELP 96-90 micelles (black). A shift in the median fluorescence is observed indicating enhanced uptake of Fn3-ELP 96-90 over ELP 96-90. Panel 3 shows the histogram of K562/WT (black) and K562/$\alpha_V\beta_3$ (gray) cells incubated with Fn3-ELP 96-90 above the CMT. A shift in the fluorescence median is observed indicating enhanced uptake for K562/$\alpha_V\beta_3$ cells.

Figure 5B. Fold increase in median fluorescence of K562/WT (gray) and K562/$\alpha_V\beta_3$ (black) cells incubated above the CMT over those incubated below the CMT. The cells were incubated with 10 μM of either Fn3-ELP 96-90 or ligand-negative ELP 96-90. K562/$\alpha_V\beta_3$ cells (black) show higher fold increase only when incubated with Fn3-ELP 96-90.

Table 1

Summary of physico-chemical and structural properties of Trx-ELP$_{BC}$ and Fn3-ELP$_{BC}$ micelles.

Protein-ELP$_{BC}$	$M_{W,app}$ (kDa)[a]	Temp (°C)[b]	R_g (nm)	R_h (nm)	ρ	Apparent aggregation number
Trx-ELP 64-60	61	45	16.2	24.0	0.68	30
Trx-ELP 64-90	75	40	19.3	27.9	0.69	76
Trx-ELP 64-120	86	40	22.3	32.2	0.69	47
Trx-ELP 96-60	75	45	21.8	28.7	0.76	48
Trx-ELP 128-60	87	45	16.7	28.0	0.60	25
Trx-ELP 96-90	86	40	25.2	30.6	0.82	87
Fn3-ELP 64-90	73	35	20.8	31.1	0.67	88
Fn3-ELP 64-120	84	35	26.5	36.6	0.72	150
Fn3-ELP 96-60	73	45	24.0	32.4	0.74	139
Fn3-ELP 128-60	85	45	18.7	31.0	0.60	69
Fn3-ELP 96-90	84	40	23.5	34.9	0.67	122

[a] Theoretical M_W of unimer

[b] Temperature of measurement